Int J Thermophys (2010) 31:1456–1465
DOI 10.1007/s10765-010-0790-0

Construction and Characterization of NTC Thermistors at Low Temperature

Yuqi Lan · Lihong Yu · Guangming Chen · Sifeng Yang · Aimin Chang

Received: 7 March 2010 / Accepted: 6 July 2010 / Published online: 23 July 2010

Abstract Nano-powder of a negative temperature coefficient (NTC) ceramic with a spinel structure of Mn–Ni–Cu–Co–La–O composition was prepared by the Pechini method. A type of NTC thermistor sensor (3.0 mm diameter × 1.5 mm high) was designed by the *in situ* lead wire attachment method (ISAM) and made using the synthesized powder. NTC thermistors were packed in the glass-sealed package. Six independent NTC thermistors were calibrated using a cryostat, a standard platinum resistance thermometer, and a Fluke 1590 super thermometer meter over the temperature range from 18 K to 120 K. The data were interpolated to obtain calibration tables at 2 K intervals from 18 K to 30 K, and at 5 K intervals from 30 K to 120 K. These tables were fitted with the equation: $1/T = A_0 + A_1 \ln(R/R_{\mathrm{ref}}) + A_2 \ln(R/R_{\mathrm{ref}})^2 + A_3 \ln(R/R_{\mathrm{ref}})^3 + A_4 \ln(R/R_{\mathrm{ref}})^4$. Aging, thermometric characteristics, fitting of calibrated data, stability of NTC thermistors, and the effect of a magnetic field on NTC thermistors were investigated.

Y. Lan (✉) · S. Yang
Beijing Institute of Aerospace Testing Technology, Beijing, China
e-mail: hangtiandiwen@163.com

L. Yu
The Key Laboratory of Cryogenics, TIPC, CAS, Beijing, China

Y. Lan · G. Chen
Institute of Refrigeration and Cryogenics, Zhejiang University, Hangzhou, China

A. Chang
The Xingjiang Technical Institute of Physics and Chemistry, Chinese Academy of Science, Urumuqi, China

Keywords Cryogenic · Electrical properties · Low temperature · Spinel · Thermistors

1 Introduction

To measure cryogenic temperatures in cryogenic experiments, various thermometers, based on various physical effects and fabricated from different materials, may be used. Resistance and diode thermometers are used widely among cryogenic ones. According to the changing resistance with temperature, resistors can be classified as having either a positive temperature coefficient (PTC) or a negative temperature coefficient (NTC). NTC resistors are normal semiconductors with a temperature dependence of resistance that decreases with increasing temperature. NTC resistors are increasingly used in various industrial and domestic applications because of their high temperature sensitivity, fast response, convenience in use, low price, etc. In addition to those advantages, they can be employed at low temperatures for high resistance to magnetic field-induced errors and ionizing radiation [1,2]. However, the price of NTC resistors prepared by the application of modern microelectronic and micromachining technologies of sensor manufacture is relatively high. Conventional manufactured thermistors for cryogenic application have a low rate of finished products, and their price is also high. In order to reduce cost, we investigated the feasibility of NTC thermistors manufactured by the technical process of common NTC thermistors [1,3–5].

NTC thermistors are semiconducting ceramics consisting of transition metal oxides with the spinel structure of the general formula $A[B_2]O_4$. In this structure, a close-packed array of oxygen ions forms a cubic lattice, where two types of lattice sites are available for the cations: a tetrahedral site (often stated as "A-site") and an octahedral site (often stated as "B-site") [6–15]. A thermally activated phonon-assisted hopping mechanism of charge carriers exists between cations of differing oxidation states on crystallographically equivalent lattice sites, which is considered as the reason for conductivity. Electrical characteristics of NTC thermistors follow the well-known Arrhenius equation: $\rho = \rho_0 \exp(B/T)$ where ρ is the specific resistivity, T is the absolute temperature, ρ_0 is the resistivity of the material at infinite temperature, and B is the thermal constant which is related to the activation energy E_a for electrical conduction according to $B = E_a/k$ (k is Boltzmann's constant) [6]. The temperature sensitivity of NTC thermistors can be described as follows: $\alpha_T = (1/\rho)(\partial\rho/\partial T) = -B/T^2$. This equation shows that the temperature sensitivity of a thermistor, α_T, has a strong dependence on the thermal constant and temperature, which decreases in temperature by a factor of T^{-2}. This suggests that there is an enormous increase in sensitivity at low temperatures [9,16]. As a result, thermistors should have low activation energy to maintain relatively moderate sensitivity at cryogenic temperatures.

Some cryogenic processes need thermometers with extreme resolution in a narrow temperature range, which also stimulated us to study Mn–Ni–Cu–Co–La oxide ceramics with those characteristics, because thermistors manufactured by those oxides have a low activation energy and can maintain high sensitivity at low temperatures. These prepared NTC thermistors were intended to be used over temperatures ranging from 18 K to 120 K.

2 Design of Thermistors

2.1 Preparation of NTC Powder Material

Mn–Ni–Cu–Co–La oxide powder was synthesized by the Pechini method. Appropriate amounts of analytical grade $Co(NO_3)_2 \cdot 6H_2O$, $Mn(NO_3)_2$, $Ni(NO_3)_2 \cdot 6H_2O$, $Cu(NO_3)_2 \cdot 3H_2O$, $La(NO_3)_3 \cdot 6H_2O$, citric acid (CA), and ethyl glycol (EG) were used as raw materials. All the nitrates were dissolved in distilled water to form mixed solutions. Then citric acid (CA) and ethyl glycol (EG) were added to the mixed solutions with a molar ratio of (metal ions):CA:EG = 1:2:2. Ammonia was dropped into mixed solutions to adjust the pH value to about three. The solution was stirred at 90 °C to form a more viscous solution, and heated to 140 °C for esterification, resulting in the formation of a resin. Upon further heating at elevated temperatures on a hot plate, spontaneous ignition of the resin occurred, resulting in a fluffy ash. The ash was milled at room temperature in a polyethylene container for 10 h, using zirconia balls as a grinding medium. The obtained cream-like mixture was dried at 80 °C, and then calcined in air at 700 °C for 2 h. The calcined oxide powder was ball-milled in ethanol for 24 h and dried.

2.2 Preparation of Thermistors

Disk-shaped thermistors were designed using the *in situ* lead-wire attachment method (ISAM). A celluloid board with a height of 2.0 mm was drilled with a row of holes with diameters of about 3.5 mm, and a distance of about 2.5 mm between holes. Then it was grooved on both sides of the centers of holes, and the distance between the two grooves with depths of 1.0 mm and widths of 0.05 mm is 2 mm. Two platinum lead wires (0.05 mm diameter) were placed into the two grooves. Granulated powders with a 4 % polyvinyl alcohol (PVA) organic binder were placed in the holes and cold-pressed to form green bodies using a steel die by single-end compaction and pressed at 200 MPa by an isopressing process. The elluloid board with the green bodies was heated in air to 400 °C at a rate of $100\,^{\circ}C \cdot h^{-1}$, kept at that temperature for 2 h for adequate binder burnout, and subsequently heated to 1100 °C at a rate of $200\,^{\circ}C \cdot h^{-1}$ and kept at that temperature for 4 h for sintering. The sintered samples were cut, and subsequently soldered to copper leads and sealed by glass. Therefore, NTC resistance sensors were manufactured. Figure 1 shows a schematic of the *in situ* lead wire attachment method (ISAM) for manufacturing thermistors.

3 Characteristics of NTC Thermistors

3.1 Aging of Thermistors

Advanced applications in the areas of medicine, consumer electronics, aerospace, and cryogenics need NTC thermistors with high reliability at extreme operating environments. To meet this high demand, the thermistor specification should be modified with

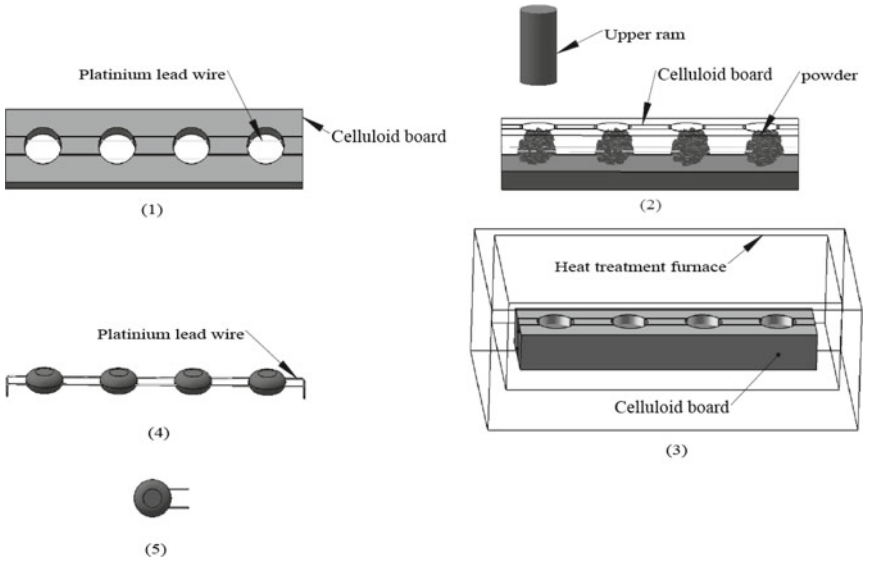

Fig. 1 Schematic of *in situ* lead wire attachment method for fabrication of thermistors

more emphasis on the reliability of the composition. The aging coefficient of the NTC thermistors is characterized by the relative variation $(R - R_0)/R_0 \times 100\ \%$, in which R_0 is the resistance value at 20 K before aging, and R is the resistance value at 20 K after aging [8,17–20]. The aging coefficient shows the long-term reliability of NTC thermistors.

Aging affects the stability. More than 20 thermistors were constructed. Resistance values of six of these NTC thermistors were measured with a 10 μA DC current at 20 K, when thermistors were placed in liquid hydrogen. Next, NTC thermistors were annealed at 100 °C for 1200 h and stored in liquid nitrogen (77 K) for 120 h. Afterward, their resistance values were again measured with a 10 μA DC current at 20 K in liquid hydrogen. The values of the aging coefficient of NTC thermistors are summarized in Table 1, ranging from 1.9 % to 4.2 %.

Table 1 R_{20K}, R_{100K} resistance, $B_{20K/100K}$ thermistor constant value, activation energy, and aging coefficient for NTC thermistor samples

Sample no.	R_{20K} (Ω)	R_{100K} (Ω)	$B_{20K/100K}$ (K)	Activation energy (eV)	Aging coefficient (%)
1	44993	11.8	205	0.0176	1.9
2	44986	11.6	207	0.0178	4.2
3	38439	12.1	202	0.0174	2.7
4	45409	12.2	206	0.0177	3.9
5	45339	11.5	206	0.0177	4.1
6	44263	11.6	206	0.0177	2.6

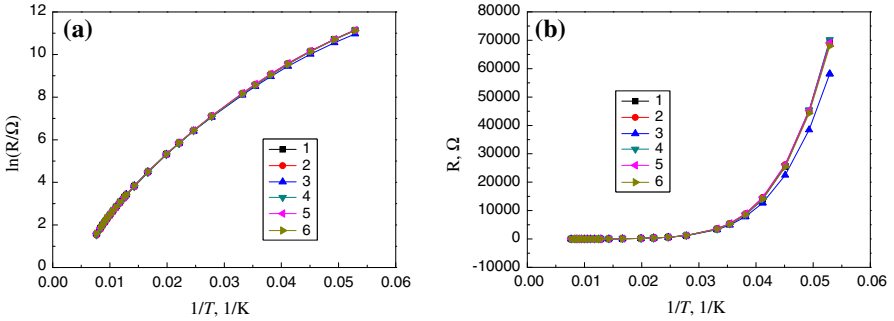

Fig. 2 Typical relationship between logarithm of resistance (**a**) and resistance (**b**) vs. inverse of absolute temperature of the six NTC thermistors

3.2 Thermometric Characteristics

A cryostat, a standard platinum resistance thermometer, and a FLUKE 1590 super thermometer meter were used for measuring the thermistors' resistance values over the temperature range from 18 K to 120 K. The six NTC thermistors were mounted, along with the standard platinum resistance thermometer, in a copper block. This block is enclosed within a quasi-adiabatic copper radiation shield, which, in turn, is thermally isolated within an outer vacuum jacket. A constant temperature of the block is achieved by an appropriately mounted heater and a precision temperature controller. All measurements were performed with a four-lead method to eliminate lead resistance. The data were interpolated to obtain calibration tables at 2 K intervals from 18 K to 30 K and 5 K intervals from 30 K to 120 K. Figure 2 shows the typical relationship between either (a) the logarithm of resistance or (b) the resistance, and the inverse of the absolute temperature of the six NTC thermistor samples. It is seen that almost all the NTC thermistor samples show linear relationships between these parameters over a wide temperature ranges, indicating good thermistor characteristics. Figure 3 shows the temperature sensitivity of NTC thermistors in the range from 18 K to 120 K. The $B_{20K/100K}$ value was calculated according to the formula $B_{20K/100K} = \ln(R_{20K}/R_{100K})/(1/T_{20} - 1/T_{100})$, where R_{20K} and R_{100K} are the resistances at 20 K and 100 K, respectively. The values of the $B_{20K/100K}$ constant and the activation energy ranged from 204 K to 207 K and from 0.0174 eV to 0.0178 eV, respectively. More specific values are summarized in Table 1.

The values of the resistance and sensitivity between manufactured NTC thermistors and other thermistors from Lake Shore Company at typical temperature are presented in Table 2. By comparing these data, it is observed that NTC thermistors have extremely high resistance and sensitivity in a narrow temperature range.

3.3 Fitting of Calibrated Data

Tables of resistance versus temperature of six NTC thermistors were established. The tables were fitted with the equation: $1/T = A_0 + A_1 \ln(R/R_{ref}) + A_2 \ln(R/R_{ref})^2 +$

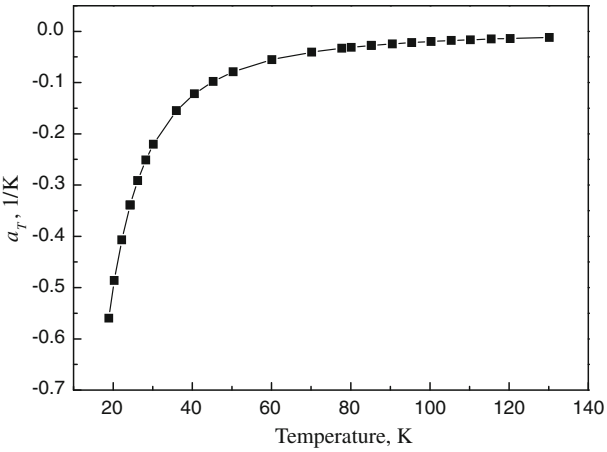

Fig. 3 Temperature sensitivity of NTC thermistors (α_T) versus temperature curve

Table 2 Values of resistance and sensitivity between NTC thermistors and different NTC RTDs from Lake Shore Company at typical temperatures

T (K)	NTC thermistors		CX-1080		GR-200A-2500		RX-102A	
	R (Ω)	dR/dT ($\Omega \cdot K^{-1}$)	R (Ω)	dR/dT ($\Omega \cdot K^{-1}$)	R (Ω)	dR/dT ($\Omega \cdot K^{-1}$)	R (Ω)	dR/dT ($\Omega \cdot K^{-1}$)
10	–	–	–	–	212.4	−69.9	1167	−15.5
20	44986	−12428	6157	−480	–	–	–	–
30	3000	−712	3319	−165	–	–	–	–
40	616	−56	–	–	6.959	−0.283	1049	−1.06
77	29	−1.8	836	−15	2.917	−0.036	–	–

$A_3 \ln (R/R_{\text{ref}})^3 + A_4 \ln (R/R_{\text{ref}})^4$ [21]. Here, R is the specific resistance, R_{ref} is 1 Ω, and T is the absolute temperature. The software, MATLAB R2006a, is used to estimate the parameters of the calibration equations. e_i is defined as follows: $e_i = T_i - \hat{T}_i$, where e_i is the error of the calibration equation, T_i is the dependent temperature variable, and $\hat{T}_i$ is the predicted values from the calibration equation. Four statistics, $e_{\max}$, $e_{\min}$, $|e|_{\text{ave}}$, and e_{std} are adopted to evaluate the precision of the equation. $e_{\max}$ is the maximum e_i value, and $e_{\min}$ is the minimum e_i value. $|e|_{\text{ave}}$ is defined as follows: $|e|_{\text{ave}} = \frac{\sum |e_i|}{n}$, where $|e_i|$ is the absolute value of e_i and n is the number of data. The uncertainty of the calibration equation can be calculated from the standard deviation of the calibration equation: $e_{\text{std}} = \left(\frac{(e_i - \bar{e}_i)^2}{n-1}\right)^{0.5}$, where $\bar{e}_i$ is the average of e_i. The estimated values of the parameters, $e_{\max}$, $e_{\min}$, $|e|_{\text{ave}}$, and e_{std} of the calibration equation for six NTC thermistors are listed in Table 3. The $e_{\max}$, $e_{\min}$, $|e|_{\text{ave}}$, and e_{std} values are relatively large. The residual plots of the calibration equation for six NTC thermistors are presented in Fig. 4. The errors are small at temperatures from 18 K to 30 K and large at temperatures from 30 K to 120 K because of the large interval for calibration

Table 3 Values of estimated parameters, e_{max}, e_{min}, $|e|_{ave}$, and e_{std} of calibration equation for six NTC thermistors

Sample no.	Parameters		e_{max}	e_{min}	$\|e\|_{ave}$	e_{std}
1	A_0	2.75×10^{-2}	36.10977	−65.4012	17.20093	24.85465
	A_1	-1.15×10^{-2}				
	A_2	3.08×10^{-3}				
	A_3	-2.66×10^{-4}				
	A_4	9.26×10^{-6}				
2	A_0	2.80×10^{-2}	41.77865	−72.5932	16.92241	25.43883
	A_1	-1.21×10^{-2}				
	A_2	3.23×10^{-3}				
	A_3	-2.90×10^{-4}				
	A_4	1.03×10^{-5}				
3	A_0	3.03×10^{-2}	28.62368	−61.1968	14.46171	20.63668
	A_1	-1.34×10^{-2}				
	A_2	3.51×10^{-3}				
	A_3	-3.13×10^{-4}				
	A_4	1.11×10^{-5}				
4	A_0	2.9×10^{-2}	32.01353	−58.1881	13.79445	20.49519
	A_1	-1.10×10^{-2}				
	A_2	2.99×10^{-3}				
	A_3	-2.64×10^{-4}				
	A_4	9.30×10^{-6}				
5	A_0	2.83×10^{-2}	32.14263	−58.0877	14.23484	21.09719
	A_1	-1.23×10^{-2}				
	A_2	3.28×10^{-3}				
	A_3	-2.95×10^{-4}				
	A_4	1.05×10^{-5}				
6	A_0	2.95×10^{-2}	27.42034	−57.5187	12.80982	19.28001
	A_1	-1.28×10^{-2}				
	A_2	3.34×10^{-3}				
	A_3	-2.94×10^{-4}				
	A_4	1.03×10^{-5}				

temperatures. Therefore, the errors, e_{max}, e_{min}, $|e|_{ave}$, and e_{std} values can be reduced if we add calibration points at temperatures from 18 K to 120 K.

3.4 Stability

The stability is the closeness of agreement between the results of the measurements of the same measure and carried out under changed conditions of measurements.

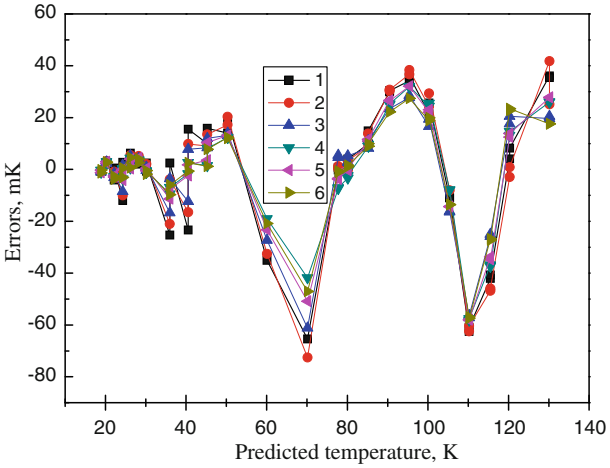

Fig. 4 Residual plots of calibration equation for six NTC thermistors

A preliminary investigation of the stability of NTC thermistors at 20 K was performed. Short-term stability data were obtained by subjecting NTC thermistors to 50 thermal shocks from ambient to liquid hydrogen. Resistance shifts were measured for each thermal cycle at 20 K by immersing the NTC thermistors in liquid hydrogen. Deviations of the NTC thermistors' resistance under thermal cycles corresponded to temperature errors in the range from 0.7 mK to 3 mK. Long-term stability data were obtained by subjecting NTC thermistors to 200 thermal shocks from 305 K to 77 K. The long-term stability for thermistors corresponded to a temperature error of not more than ± 10 mK at 20 K. Compared with germanium, Cernox™, and ruthenium oxide (Rox™) RTDs, the stability of NTC thermistors may be much better.

3.5 Effect of Magnetic Field on NTC Thermistors

In some cryogenic engineering and physics applications, there is a demand for measurements of temperature in magnetic fields. In order to gain accurate temperature measurements in the presence of magnetic fields, it is very important to develop special cryogenic thermometers [1,4,5]. In the application processes of thermometers, any magnetic field change results in a deviation in the temperature measurement. The magnitude of these errors substantially depends on the properties of the material. Therefore, different thermometers exhibit different behaviors in magnetic fields. The error in thermometer readings, induced by magnetic fields, can be characterized by the variation, $dT = T(B) - T$, for which T is the temperature measured at magnetic field $B = 0$, and $T(B)$ is the temperature measured at magnetic field B. NTC thermistors were measured by immersing them in liquid nitrogen (77 K) and in liquid hydrogen (20 K). The magnetic field-dependent temperature errors dT/T for NTC thermistors at various magnetic fields and temperatures are displayed in Fig. 5. Typical magnetic field-dependent temperature errors, dT/T (%), of different sensors at B

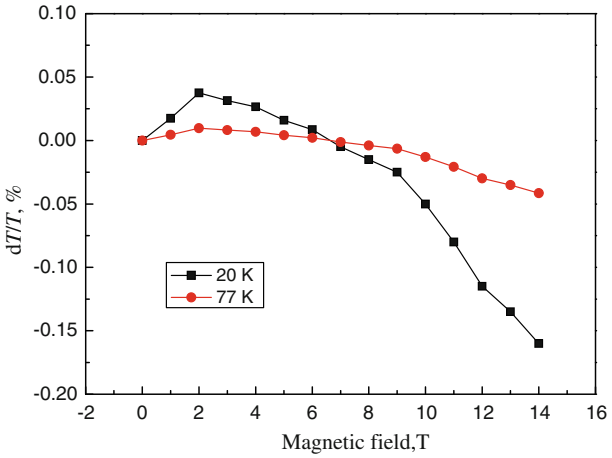

Fig. 5 Temperature errors, dT/T (in %), versus magnetic field curves for NTC thermistors

Table 4 Typical magnetic field-dependent temperature errors, $dT/T(\%)$, of different sensors at B (magnetic induction)

T (K)	Types of sensors	2.5 T	8 T	14 T
20	NTC thermistors	0.035	−0.015	−0.12
	CX-1050	0.04	0.02	−0.16
	GR-200A-250	–	–	–
30	NTC thermistors	–	–	–
	CX-1050	0.01	0.04	0.06
	GR-200A-250	0.2	0.2	0.3
77	NTC thermistors	0.007	−0.004	−0.04
	CX-1050	0.002	0.022	0.062
	GR-200A-250	<0.1	<0.1	0.17

(magnetic induction) are listed in Table 4. As a result, manufactured NTC thermistors are excellent for use in magnetic fields.

4 Conclusions

NTC thermistors, based on an Mn–Ni–Cu–Co–La oxide, have been designed and manufactured for use in the temperature range from 18 K to 120 K. They showed good electrical properties, stability, and high resistance to magnetic field-induced errors at operating temperatures, which might be useful from the standpoint of fabricating accurate cryogenic sensors, of expanding the operating temperature of cryogenic sensors, of cutting down losses, and of reducing the effect of magnetic fields. Therefore, their widespread application is important in cryogenic engineering.

Acknowledgments This study was supported in part by the Material Physics and Chemistry Research Center of the Xingjiang Technical Institute of Physics and Chemistry, the Chinese Academy of Science. The authors are grateful to Wei Wang for careful preparation and Anguang Huang for measuring the electrical data and aging of samples.

References

1. B.L. Brandt, D.W. Liu, L.G. Rubin, Rev. Sci. Instrum. **70**, 104 (1999)
2. C.C. Wang, S.A. Akbar, W. Chen, J.R. Schorr, Sens. Actuators A **58**, 237 (1997)
3. V.F. Minti, Mol. Phys. Rep. **21**, 71 (1998)
4. C.J. Yeager, S.S. Courts, IEEE Sens. **1**, 352 (2001)
5. E.F. Venager, N.S. Boltovers, M. Oszwaldowsiki, T. Berus, Sens. Actuators A **68**, 303 (1998)
6. C. Metzmacher, R. Mikkenie, W.A. Groen, J. Eur. Ceram. Soc. **20**, 997 (2000)
7. M. Vakiv, O. Mrooz, I Hadzaman, J. Eur. Ceram. Soc. **21**, 1783 (2001)
8. D.-L. Fang, C.-S. Chen, A.J.A. Winnubst, J. Alloys Compd. **454**, 286 (2008)
9. A. Rousset, R. Legros, A. Lagrange, J. Eur. Ceram. Soc. **13**, 185 (1994)
10. E.G. Larson, R.J. Arnott, D.G. Wickham, J. Phys. Chem. Solids **23**, 1771 (1962)
11. F. Golestani-Fard, S. Azimi, K.J.D. Mackenzie, J. Mater. Sci. **22**, 2847 (1987)
12. V.A.M. Brabers, F.M.V. Setten, P.S.A. Knapen, J. Solid State Chem. **49**, 93 (1981)
13. O. Mrooz, A. Kovalski, J. Pogorzelska, O. Shpotyuk, M. Vakiv, B. Butkiewicz, J. Maciak, Microelectron. Reliab. **41**, 773 (2001)
14. J.G. Fagan, V.R.W. Amarkoon, Am. Ceram. Soc. Bull. **72**, 70 (1993)
15. K. Park, S.J. Kim, J.-G. Kim, S. Nahm, J. Eur. Ceram. Soc. **27**, 2009 (2007)
16. A. Banerjee, S.A. Akbar, Sens. Actuators A **87**, 60 (2000)
17. R. Metz, J. Mater. Sci. **35**, 4705 (2000)
18. M.M. Vakiv, O.I. Shpotyuk, V.O. Balitska, B. Butkiewiez, L. Shpotyuk, J. Eur. Ceram. Soc. **24**, 1243 (2004)
19. W.A. Groen, C. Metzmacher, P. Huppertz, S. Schuurman, J. Electroceram. **7**, 77 (2001)
20. B. Gillot, M. Kharroubi, R. Metz, R. Legros, A. Rousset, Solid State Ionics **44**, 275 (1991)
21. C. Chiachung, Measurement **42**, 1103 (2009)